

Planning and Deployment of WiMAX Networks

Pedro Sebastião · Fernando José Velez · Rui Costa ·
Daniel Robalo · António Rodrigues

Published online: 26 August 2009
© Springer Science+Business Media, LLC. 2009

Abstract Incorporation of measurement based techniques in Worldwide Interoperability for Microwave Access (WiMAX) are required to improve IEEE 802.16 engineering methodologies. Wireless planning methodologies are presented, supported by a planning tool which facilitates the design and implementation of WiMAX networks. Propagation models available for WiMAX still need to be tuned and further validated. By comparing IEEE 802.16-2004 measurement results at 3.5 GHz with computed values using the modified Friis and the Stanford University Interim (SUI) models, for a suburban area, we found that the use of the modified Friis equation with a propagation exponent ~ 3 is more appropriate than the use of the SUI model, although, for coverage distances between 275 and 475 m, the SUI-B and mainly SUI-C models may still be used. From the analysis of the carrier-to-noise-plus-interference ratio, it is clear that both noise and interference present a strong limitation to the cellular reuse performance of fixed WiMAX mainly for higher order modulation and coding

P. Sebastião
Instituto de Telecomunicações/Lisbon University Institute-ISCTE/Instituto Superior Técnico,
Av. Rovisco Pais, 1, Torre Norte, 1049-001 Lisboa, Portugal
e-mail: pedro.sebastiao@iscte.pt

F. J. Velez (✉) · R. Costa · D. Robalo
Instituto de Telecomunicações-Department of Electromechanical Engineering,
Universidade da Beira Interior, Calçada Fonte do Lameiro, 6201-001 Covilhã, Portugal
e-mail: fjv@ubi.pt

R. Costa
e-mail: ruicosta@fcsaude.ubi.pt

D. Robalo
e-mail: robalo_daniel@hotmail.com

F. J. Velez
Centre for Telecommunications Research, King's College London, Strand, London WC2R 2LS, UK

A. Rodrigues
Instituto de Telecomunicações/Instituto Superior Técnico, Av. Rovisco Pais, 1, Torre Norte,
1049-001 Lisboa, Portugal
e-mail: antonio.rodrigues@lx.it.pt

schemes. With a reuse pattern $K = 7$, cell throughputs near the maximum are only achieved in the uplink if sub-channelisation is used together with sectorization. The planning tool provides planners with practical and useful information through quick coverage/capacity based procedures, and outputs the number and position of the base stations and an estimation of the total cost of implementation, based on data provided by different equipment manufacturers. WiMAX cellular planning exercises are presented for the zone of Covilhã, Portugal, where Geographic Information Systems are used for representation of rural and sparse urban areas. One of the main conclusions is the strong need to use sector antennas in order to guarantee an adequate coverage, and higher system capacity whilst mitigating interference for several terrain types and environments, including hilly terrain.

Keywords Network communications · Mobile communication systems · Public networks · Wireless communication

1 Introduction

Presently telecommunications systems provide the opportunity to use Worldwide Interoperability for Microwave Access (WiMAX) based technologies, since they support mobile broadband Internet services in outdoors (and even in indoor, for the lower frequency bands) with high coverage ranges and user mobility support. They also allow the exchange of truly wide and broadband multimedia content, and support simultaneously all Internet Protocol (IP) voice, data, streaming, image and video multi-rate communications.

WiMAX is the commercial name for IEEE 802.16. In terms of standardisation, the IEEE 802.16-2004 group is dedicated to Point-to-Point (PtP) and Point-to-Multipoint (PtM) networks (without mobility support) while the IEEE 802.16e group is dedicated to PtM networks that support mobility. WiMAX uses Orthogonal Frequency Division Multiplexing (OFDM), Orthogonal Frequency Division Multiple Access (OFDMA) and dynamic modulation scaling, i.e., the system is able to adapt itself to the best modulation/coding schemes, taking into account carrier-to-noise-plus-interference (*CNIR*) versus physical throughput constraints [1].

Channels of 3.5, 7 and 10 MHz are defined in IEEE 802.16-2004. As link distances of the order of tens of kilometres can be guaranteed, WiMAX is a good solution for broadband backhauling, up to 50 km (in the PtP case) and cell coverage radius between 2 and 5 km (in the PtM case).

The goal of cellular coverage is to provide access to mobile users within a given zone, called cell while guaranteeing the quality of the received signal in both directions, uplink (UL) and downlink (DL), even for the users at cell boundary. As resources, e.g., frequency channels, need to be reused in different geographical zones (but not in close proximity), the impact of interference among co-channel cells needs to be evaluated also in both directions. In WiMAX, as in Universal Mobile Telecommunications System (UMTS) and High Speed Downlink Packet Access (HSDPA), the ideal situation would be to reuse the channels in every cell, i.e., to deploy systems with a frequency pattern, K , equal to one, which would be achieved by means of Pseudo Random Mapping (PRM) of sub-carriers where OFDMA is used. However, due to heavy interference in frequency reuse deployment, users at the cell edge may suffer from low connection quality since these improvements may not be available in some versions of the standard, or may simply reduce but not eliminate interference.

In the context of WiMAX cellular deployment and planning, research on the variation of the carrier-to-noise-plus-interference ratio with different system parameters is therefore of paramount importance, and techniques such as sub-channelisation need to be explored.

In the south of Europe, the introduction of WiMAX gains special interest for emergency and security public services. For example, in Summer time, forest fires are a persistent calamity, and authorities lack access to real-time fire information in order to coordinate fire brigades. For demonstration a network was deployed in the city of Covilhã, Portugal using IEEE 802.16-2004 equipment with 3.5 MHz channels at 3.5 GHz [2] supporting eight different Modulation and Coding Schemes (MCSs). However, only with the use of IEEE 802.16e standard [3] true mobility will be supported. Different received power levels correspond to different net Physical (PHY) bit rates and to MCSs. This PtM network is the basic tool for our research in broadband mobile access, mobile IP, and always best connected WiMAX scenarios, including the possibility of performing extensive field trials in the frequency division duplexing (FDD) mode.

In order to automate the cellular planning process, graphical planning tools that account for terrain profile need to be applied. In a previous version of the planning tool presented in [4], the so-called Wireless Planning Tool (WPT) addressed only the IEEE 802.11 Wi-Fi standards [5]. In this paper, fixed WiMAX functionalities have been incorporated in the new platform. For a given coverage region and expected user capacity, the WPT estimates the position of APs leading to the lowest cost, based on data provided by manufacturers. There are other tools in the market for Wi-Fi and/or WiMAX planning which involve higher complexity and costs [6–9] but do not include both technical and economic/budget issues as in this version of the WPT.

The remaining of this paper is organized as follows. Section 2 addresses outdoor propagation models. IEEE 802.16-2004 equipment 3.5 GHz, was used to compare measurements with the theoretical values for the modified Friis and Stanford University Interim (SUI) propagation models. In Sect. 3, the trade-offs regarding carrier-to-noise-plus-interference ratio are addressed. As the existence of obstacles, e.g., mountains, trees and buildings can affect line-of-sight propagation, Geographic Information System (GIS) based dimensioning is used for rural and sparse urban areas, in mixed hilly/flat zones. Section 4 presents the WiMAX cellular planning framework and scenario, highlights the functionalities and potentialities of the WPT, and discusses the results. Finally, conclusions are presented in Sect. 5.

2 Outdoor Propagation Models

2.1 SUI Versus Modified Friis

In Non Line-of-Sight (NLoS) channel conditions, signals may undergo scattering, diffraction, polarization changes and reflection impairments, which affect their level and phase at the receiver. Usually these impairments are not important when there is Line-of-Sight (LoS) between the transmitter and the receiver.

For outdoor environments, obstacles, such as buildings materials, foliage, and clutter, also contribute to increase path loss [10, 11]. In this context, the SUI outdoor propagation model is especially relevant [11], and it will be considered together with the modified Friis model.

Over the years, various models have been developed to characterize Radio Frequency (RF) environments and allow for the prediction of the RF signal strengths. These empirical models are used to predict large-scale coverage for radio communications systems in cellular applications and provide estimates for Path Loss (PL) by considering the transmitter/receiver distance, terrain factors, antenna height, and cellular frequencies. Nevertheless, according to [11] none of these models address the needs of broadband fixed wireless adequately, thus

providing the rationale to develop the SUI model. This model is used in the IEEE 802.16 standard and is described in [12]. The wireless PL model includes, as parameters, antenna heights, carrier frequency and types of terrain [11]. Apart from the modified Friis model (where the propagation exponent γ takes an empirical value other than 2), one possible solution is therefore the SUI model, which is an extension of earlier wireless propagation models [11].

The SUI model considers three basic terrain types:

Category A—Hilly/moderate-to-heavy tree density;

Category B—Hilly/light tree density or flat/moderate-to-heavy tree density;

Category C—Flat/light tree density.

These terrain categories provide a simple method to estimate more accurately the PL of the RF channel in an NLoS situation. Being statistical in nature, the model is able to represent the range of PLs experienced within an actual RF link. SUI propagation models were explored for the design, development and testing of WiMAX links in six different scenarios, SUI-1 to SUI-6 [13]. By using these propagation models, it is then possible to predict more accurately the coverage probability achieved within a base station site sector. Although these models do not replace detailed site planning (and site surveying) they may provide an estimate before actual planning of the network. Besides, it is very important to perform RF planning activities to adequately evaluate specific environment factors, co-channel interference, actual clutter and terrain effects.

This model allows several frequencies and subscriber station (SS) heights. The path loss is given (in dB) by [10]

$$PL(d) = \overline{PL}(d_0) + 10 \cdot \gamma \cdot \log_{10}(d/d_0) + X_f + X_h + S \quad (1)$$

where $\overline{PL}(d_0)$ is the standard path loss for a distance d_0 from the non-modified Friis model, and

$$\gamma = a - b \cdot h_b + c/h_b, \quad (2)$$

where d is the distance between the Base Station (BS) and a given point, in meters, $d_0 = 100$ m, $\lambda = c/f$ is the wave length, $c = 3 \times 10^8$ ms⁻¹, f is the carrier frequency, h_b is the BS height above ground, in meters ($10 < h_b < 80$ m), and a , b and c are parameters which are chosen according to three terrain types, represented by A, B or C, Table 1. The terms X_f and X_h are correction factors for frequency and SS antenna height above the ground, respectively.

These correction factors are defined as

$$X_f = 6.0 \cdot \log(f/2000) \quad (3)$$

and

$$X_h = \begin{cases} -10.8 \cdot \log(h_m/2.0), & \text{for terrain types A and B} \\ -20.0 \cdot \log(h_m/2.0), & \text{for terrain type C} \end{cases} \quad (4)$$

where f is the carrier frequency, in MHz, and h_m is the receiver height above the ground, in meters. The term S is a lognormal-distributed random variable, with zero mean and standard deviation σ_S , with typical values from 8.2 to 10.6 dB, depending on the type of terrain [10]. This term takes shadow fading originated by trees and structures into account [10].

The average received power is given by $\overline{PR}(d) = \overline{PE} - \overline{PL}(d)$, where \overline{PE} is the average transmission power, and $\overline{PL}(d)$ is the average path loss (attenuation factor).

Table 1 Values for the parameters in the SUI model

Model constant	Terrain type		
	A	B	C
<i>a</i>	4.6	4.0	3.6
<i>b</i>	0.0075	0.0065	0.0050
<i>c</i>	12.6	17.1	20

In the other commercially available cellular planning tools, models with high complexity can be used, namely, the NLoS dominant ray path loss one [10, 14]. However, in order to obtain the most efficient cellular planning tools, it is important to compare these models with the simplest ones, e.g., the modified Friis and SUI model, and validate them against experimental results.

2.2 Experimental Results

Figure 1 presents some of the PtM Alvarion WiMAX equipment used in the experimental setup installed on the roof top of the Health Sciences Faculty (HSF) of University of Beira Interior, Covilhã, near the Hospital.

They are a BreezeMAX 3000 OFDM micro BS and self-installable Alvarion BreezeMAX Customer Premise Equipments (CPEs) operating at 3.5 GHz. The omnidirectional BS antenna and the Outdoor Unit (ODU) are shown in the left picture while the BS and CPE are presented in the right hand side ones. The appropriate Ethernet and RF cables were also used, as well as a Global Positioning System (GPS) device, a 12–240 V power inverter (to feed the CPE), and a portable PC, used as a terminal and running a File Transfer Protocol



Fig. 1 IEEE 802.16-2004 PtM equipment operating at the experimental setup

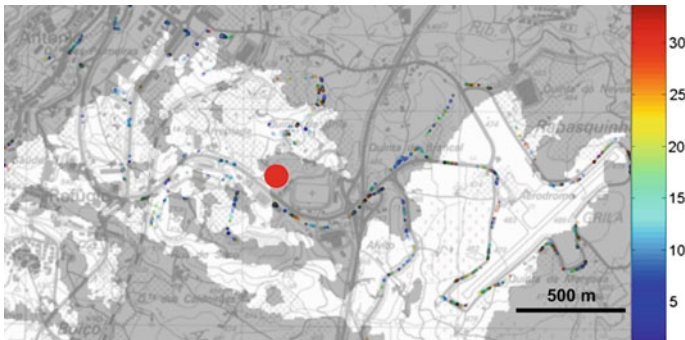


Fig. 2 Measurements of $SNR_{[dB]}$ at 3.5 GHz in the DL (NLoS regions are represented in grey)

(FTP) application, the BreezeCONFIG software, and a tool for acquiring GPS positions. In the HSF backhaul network, there was an FTP server, and a Dynamic Host Configuration Protocol (DHCP) server, for automatically assigning an IP address to the users' CPEs. The BS antenna gain is 10 dBi (360° azimuth, 8° elevation, vertical polarization). The SS antenna is a beam switching array of six 9 dBi, 60° antennas, integrated into the CPE.

Field trials were performed in the suburban area of Covilhã, in a zone with approximately $2.80 \times 1.55 \text{ km}^2$, and initial results for the Signal-to-Noise Ratio, SNR , and the throughput were obtained at the SSs (or CPEs) that roam around the suburban area surrounding the HSF. The dynamic range of the CPE was found to be adequate. The BreezeMAX duplexing frequency range is 3499.5–3553.5 MHz and 3550–3600 MHz for Downlink (DL), and 3399.5–3453.5 MHz, and 3450–3500 MHz for Uplink (UL) [8]. In these particular field tests, our ODU was operating at 3551.75 MHz (DL), and 3451.75 MHz (UL). ODU transmitter power was 28 dBm. There is a direct correspondence between the SNR values from Fig. 2, the achieved MCSs, and data rate, e.g., $\sim 6 \text{ Mbps}$ for 16-QAM.

NLoS regions, obtained with ArcGIS, are represented in the background, in grey, in Fig. 2. At distances far from the base station, the experimental regions with reasonable signal quality coincide basically with the LoS regions. However, for distances up to $\sim 550 \text{ m}$ even NLoS areas near the boundary between LoS and NLoS areas can be covered.

Another important issue is the comparison between the results for curve fitting of SNR , or carrier-to-noise ratio (C/N) and the curves obtained from the application of the propagation models (SUI model and modified Friis equation), as depicted in Fig. 3, for distances up to $\sim 1.6 \text{ km}$.

Within the modified Friis model different propagation environments are modelled by different propagation exponents, γ , which vary from $\gamma = 2$, corresponding to free space conditions, e.g., rural areas, to $\gamma = 3$, in urban areas (no shadowing), and $\gamma = 4$, in shadowed urban areas [15, 16]. For the SUI model [11], one considers $h_m = 2 \text{ m}$, $h_b = 13.3 \text{ m}$ and $\sigma_\gamma = 8.8 \text{ dB}$. For both models, total antenna gain (transmitter plus receiver) of 19 dBi, a radio frequency bandwidth $b_{r,f} = 3.5 \text{ MHz}$, and a noise factor $N_f = 3 \text{ dB}$ were used.

To understand the results, an analysis of the terrain profile around the BS location at HSF is required. While at Southeast (SE) of the BS the terrain is flat, at Northwest (NW) it is continuously hilly, with increasing altitudes. In Fig. 2 the crown with a radius of $\sim 550 \text{ m}$ from the BS is part of the suburban region of Covilhã, with a moderate building density. The second crown, for distances larger than 550 m, corresponds to a rural area at SE, and to a dense urban area at NW. However, this urban area corresponds to zones predominantly in

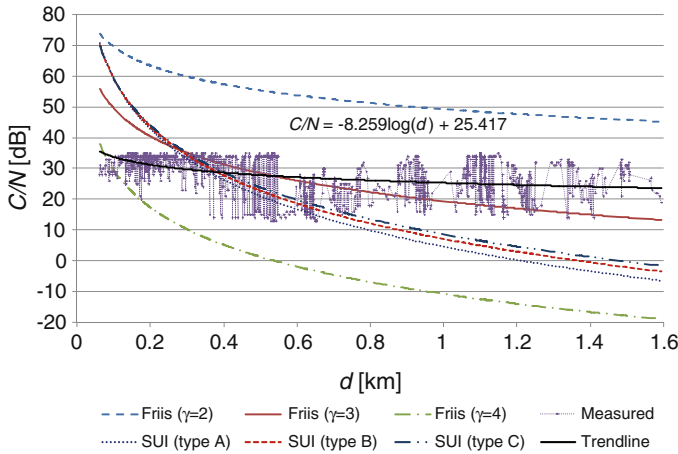


Fig. 3 Trend curve for the measured SNR in the locations around HSF-UBI: comparison between the SUI and the modified Friis models

LoS with the BS as the terrain height continuously increases from the BS to this zone. At SE, the zones up to a distance of ~550 m are predominantly in NLoS due to the shadowing effect of the roof. However, at NW of the BS, this crown is predominantly covered with LoS (as for longer distances), as the terrain height increases. For distances larger than 550 m measurements were taken mostly with LoS coverage.

A curve fitting approach was used to interpret measurement results from Fig. 3 (in dB). The coefficient -8.259 for $\log(d)$ corresponds to a very low power decay rate. If the modified Friis equation is considered, the experimental results take values similar with the curve for $\gamma = 4$ for distance in the interval [60, 150] m, similar to the ones from the curve for $\gamma = 3$ for distances in the interval [300, 500] m. Then, for larger coverage distances, values correspond to modified Friis equation propagation exponents between 2 and 3. It seems that the results consecutively correspond to (1) shadowed urban areas, (2) urban areas (with no shadowing), and (3) approximately free space, which partially agrees with the actual terrain. Unlike the SUI model, in this case, distances shorter than 100 m are considered.

Despite the fact that use of the SUI model is recommended for WiMAX, the comparison of experimental results with the SUI model is harder since they only coincide for distances in the interval [275, 475] m. In order to clarify this issue, Fig. 4 presents a partial analysis of the results for C/N in this interval, where a different trendline is considered, and only the modified Friis equation curve for $\gamma = 3$ is considered for comparison, as it approximately follows the experimental trendline for the results with a difference of circa 2.5 dB (which can be caused by the penetration loss due to the placement of the SS antenna in the rear seat of the car during the measurements).

If this difference of 2.5 dB was discounted from results for modified Friis equation with $\gamma = 3$, the curves would be almost coincident. This was confirmed by the reduction of the mean square error (MSE) from 4.917 to 0.113.

Without this correction factor, while the distance to the BS increases, the trendline consecutively crosses the curves for SUI-A, SUI-B, and SUI-C, i.e., the curves for (a) hilly/moderate-to-heavy tree density, (b) hilly/light tree density or flat/moderate-to-heavy tree density, and (c) flat/light tree density, respectively. The experimental results cross the three curves of the SUI model but a good correspondence was only found for the SUI-B and

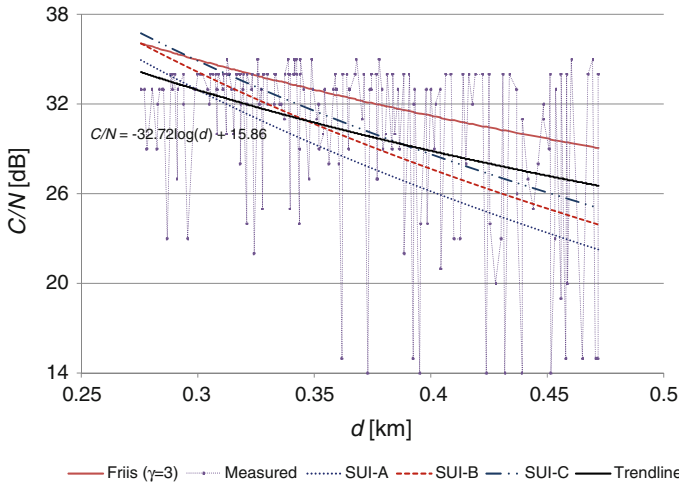


Fig. 4 Analysis of the measured SNR for distances in the interval [275, 475]m: comparison between the SUI and the modified Friis models

SUI-C, as the MSE is 1.564 and 1.617, respectively. For the SUI-A curve the mean square error was 4.657. However, if we apply the correction factor of 2.5 dB (as for the modified Friis equation) the results for the SUI-A and SUI-B models would be much worst (MSE of 19.227 and 9.247, respectively). Only the curve for the SUI-C would still offer an almost acceptable correspondence (with an MSE of 4.808).

3 Carrier-to-Noise-Plus-Interference Ratio

In order to achieve an efficient use of the radio frequency spectrum, it is important to choose a frequency reuse scheme that leads to full coverage guarantee and improved system capacity whilst minimising the interference. In WiMAX, the achievable user physical throughput is a function of the supported MCS which, in turn, depends on the values of the achievable CNIR. It is therefore important to analyse the evolution of CNIR with the distance and with several system parameters.

If frequency division duplexing (FDD) is used in fixed WiMAX, an analytical approach may be followed to solve coverage and frequency reuse problems. Worst-case situations occur in the DL when the BS transmits to the SS, located at the cell edge, whilst receiving interference from the BSs of the six co-channel cells of each ring of interference at a distance D (the reuse distance). Previous research on intercell interference in broadband wireless access is addressed in [17, 18]. In the UL, the worst-case situation occurs when the SS is transmitting to the BS from the cell boundary, while interfering mobiles are at the interfering cells boundary (in the region closest to the central cell), at a distance $D-R$ (where R is the coverage distance). When sectorization is considered the number of interfering cells is decreased, and system capacity increases.

As there would be limitations arising from an independent analysis of the carrier-to-noise and the carrier-to-interference ratios, cellular planning has to consider simultaneously both constraints [19, 20]. CNIR is taken into account by assuming that the weights for noise and interference are the same.

The modified Friis propagation model with $\gamma = 3$, transmitter power $P_t = -2$ dBW, transmitter and receiver antenna gains, $G_t = 17$ dBi and $G_r = 9$ dBi, respectively, were assumed. Note that transmitter antenna gain is 7 dB higher than the value considered in Sect. 2. Radio frequency bandwidth were the same as in Sect. 2.

Since sub-channelisation in the IEEE 802.16-2004 UL is an optional feature, we explored its impact on the achieved MCS. Differently from the mobile version of WiMAX, IEEE 802.16-2004 only supports sub-channelisation in the UL. It limits SS transmissions to 1/16 of the bandwidth assigned to the UL communication to the BS. The standard defines 16 sub-channels, and 1, 2, 4, 8 or all sets of sub-channels can be assigned to a SS. Each user in a different sub-channel may use a different MCS in a flexible way as far he/she is using a different sub-channel.

To better understand the changes caused by sub-channelisation (16 sub-channels) and sectorization it is worthwhile to plot charts for $CNIR$ as a function of the co-channel reuse factor, r_{cc} , with R as a parameter.

The power of the carrier at the receiver is obtained by computing the power received by an SS at a distance R from the BS. The computation of the interference depends on the UL and DL configurations, and on the use of sectorization as well. The required equations are given in [21].

In fixed WiMAX, an important comparison is between absence and presence of sub-channelisation in the UL. Another important case is the simultaneous use of sub-channelisation and sectorization.

From these charts, considering the C/N thresholds for each MCS, i.e., $(C/N)_{\min}$, it is straightforward to obtain the achievable physical cell throughput, not considering the mixture of services and applications, and the corresponding “multiplexing” characteristics. These charts allow exploring what the achievable $CNIR$ and throughput for a given reuse pattern, K . As, for hexagonal-shaped cells, $K = 7$ corresponds to a reuse factor $r_{cc} = 4.58$ we considered this value as a goal. Since the supported system capacity depends on r_{cc} , it is worth to represent the dependence of $CNIR$ on r_{cc} . We are aware that, for the cases where sub-channelisation is considered in Fixed WiMAX, the approach we follow for $CNIR$ does not cope with per sub-channel equivalent SINR (or $CNIR$) computations. These computations can be performed accounting either for exponential effective SINR mapping (EESM), effective code rate map (ECRM), or mean instantaneous capacity (MIC), and may be applied in the future to improve the relevance of the $CNIR$ curves through the use of one of these compression techniques.

Figure 5 shows $CNIR$ as a function of r_{cc} with R as a parameter for the UL while Fig. 6 presents the corresponding variation of the achievable throughput with r_{cc} for each MCS. The WiMAX equipment uses eight different MCS with different $CNIR$ thresholds, Table 2.

It is clear that for $r_{cc} = 4.58$, values of $CNIR$ are always lower than 8.9 dB, and that for coverage distances larger than 2 km they decrease drastically. As a consequence, for $r_{cc} = 4.58$, the achievable physical throughput is very low ($R_b = 2.82$ Mbps maximum) compared with the maximum achievable, i.e., 12.27 Mbps, Fig. 6.

Although the results are not presented here the following conclusions were also made: (1) for the DL the results are better, and a value of the physical throughput of 4.23 Mbps is achieved for distances up to 2 km; (2) with sub-channelisation, improvements are only evident for the highest coverage distances, i.e., the main improvement is on the coverage.

If sectorization is applied alone then the values for $CNIR$ at $r_{cc} = 4.58$ will be higher. However, a truly improvement for coverage distances up to 3 km (not only up to 2 km anymore) requires both sectorization and sub-channelisation for the UL, Fig. 7. For these values of r_{cc} and R , the values of $CNIR$ exceed 15 dB. This clearly confirms the need to use both improvement techniques simultaneously.

Fig. 5 *CNIR* as a function of r_{cc} with R as a parameter, for the UL, no sub-channelisation

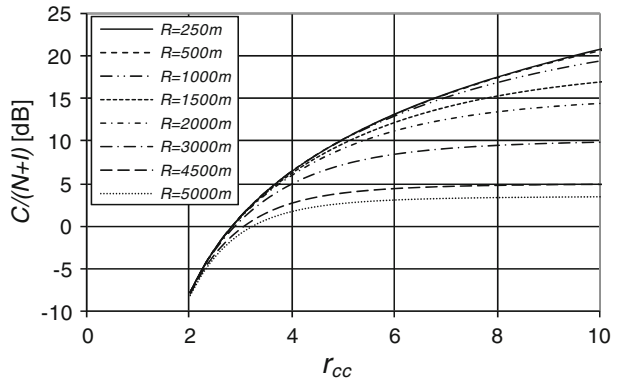


Fig. 6 Physical throughput as a function of r_{cc} with R as a parameter, for the UL, no sub-channelisation

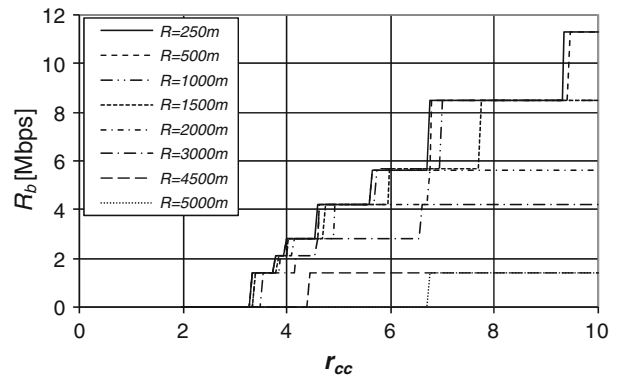


Table 2 Correspondence between MCSs, minimum *CNIR* and the physical throughput

ID	MCS	<i>CNIR</i> _{min} (dB)	Physical throughput (Mbps)
1	BPSK 1/2	3.3	1.41
2	BPSK 3/4	5.5	2.12
3	QPSK 1/2	6.5	2.82
4	QPSK 3/4	8.9	4.23
5	16-QAM 1/2	12.2	5.64
6	16-QAM 3/4	15.0	8.47
7	64-QAM 2/3	19.8	11.29
8	64-QAM 3/4	21.0	12.27

Improvements in the analysis may be obtained with the assessment of the achievable throughput, R_b , as function of the distance within a cell when the coverage distance (or cell radius) takes a given value, e.g., $R = 2$ or 3 km. For a fixed r_{cc} , since higher coverage distances imply limitations on coverage but less interference, it is important to compare the achievable maximum throughput for a given value of the reuse pattern, e.g., $K = 7$, for each value of the distance, d , from the BS to an SS, and each MCS. Different values are considered for the coverage distances, R .

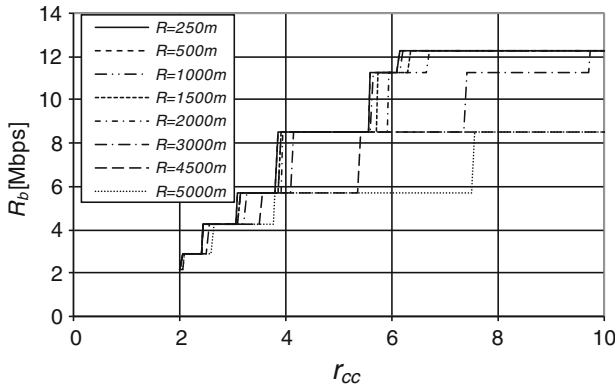


Fig. 7 Physical throughput as a function of r_{cc} , with R as a parameter, for the UL, with sub-channelisation and sectorization

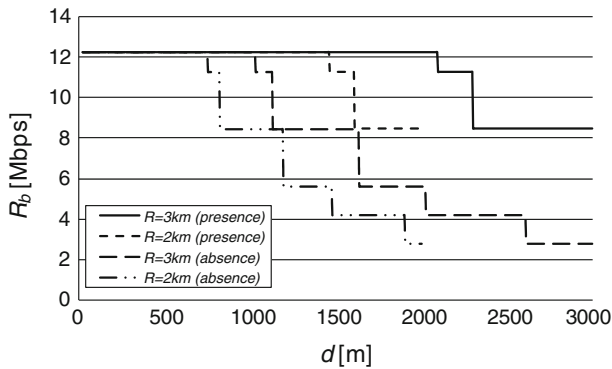


Fig. 8 Maximum achievable physical throughput as a function of d for $K = 7$, and for $R = 2$ and 3 km for the UL, in the absence and presence of sub-channelisation/sectorization

In the omnidirectional case, while the power of the received carrier is computed for a distance d , the distances for the computation of interference can be maintained, i.e., $r_{cc} \cdot (R - 1)$ for the UL and $\sim r_{cc} \cdot R$ for the DL. In the tri-sectorial case, the power of the received carrier is also computed for a distance d , but in the computation of interference the following formulation stands

$$C/I = \frac{d^{-\gamma}}{(r_{cc} \cdot R + 0.7 \cdot d)^{-\gamma} + (r_{cc} \cdot R - 0.22 \cdot d)^{-\gamma}} \tag{5}$$

Figure 8 presents the maximum achievable throughput as a function of d for $K = 7$ for the UL, in the absence of sub-channelisation and sectorization, $0 \leq d \leq R$. A similar analysis was also performed for the DL, and better results were achieved. Although the results are not presented here, for a fixed K , with the use of sectorization (tri-sectorial 120° antennas) there is a clear increase on the distances for which the highest values for the throughput are achievable.

Figure 8 also presents results for the maximum distances up to which MCS may be used with sub-channelisation and sectorization (tri-sectorial 120° antennas). Using these values for the distance, and applying a simple equation to compute the areas it is possible to obtain the size of the multiple rings where it is possible to support each MCS.

Table 3 Average cell throughput for $R = 2$ and 3 km

R_{b-av} (Mbps)	$R = 2$ km			$R = 3$ km		
	No sub-channelisation		With sub-channelisation	No sub-channelisation		With sub-channelisation
	DL	UL	UL	DL	UL	UL
Omnidirectional	7.624	6.473	6.803	6.753	5.886	6.751
Sectorial	9.664	9.664	10.808	7.756	7.756	10.605

Table 3 presents the results for the average of maximum throughput obtained by combining the results for the throughput with the ones for the size of the covered area for both link directions, with and without the use of sub-channelisation. For a fixed K , the use of sub-channelisation improves the coverage slightly. Only sectorization clearly increases the achievable throughput. Furthermore, the simultaneous use of sub-channelisation and sectorization clearly benefits the use of the highest level MCSs for coverage distances larger than in the remaining cases.

Without sectorization, while for $R = 2$ km the consideration of sub-channelisation only leads to an increase in UL throughput of 4.8%, from 6.473 to 6.803 Mbps, for $R = 3$ km the increase reaches 15.1%, from 5.886 to 6.751 Mbps. For $R = 3$ km the use of sub-channelisation leads to an almost perfect balance between the DL and UL whilst for $R = 2$ km this improvement does not occur.

With sectorization, while for $R = 2$ km the consideration of sub-channelisation leads to an increase in throughput in the UL of 11.84%, from 9.664 to 10.808 Mbps, for $R = 3$ km the increase is 36.73%, from 7.756 to 10.605 Mbps. In this case, with the use of sub-channelisation, UL throughput clearly surpasses DL throughput.

Therefore, both noise and interference present strong limitations to the cellular reuse performance of fixed WiMAX, mainly for higher order MCSs. As a consequence, with a reuse pattern $K = 7$, cell throughputs near the maximum are only achieved in the UL if sub-channelisation is used together with sectorization due to the simultaneous decrease of the noise power and the mitigation of interference through sectorization.

In the omnidirectional case, with the use of sub-channelisation, although the noise power decreases, the improvement only allows for a balance of the physical throughputs between the UL and DL for $R = 3$ km. Nevertheless, these relative improvements are not achieved for $R = 2$ km.

The use of sectorization reduces the interference, and an improvement on the achievable physical throughput of $\sim 59\%$ is obtained for $R = 2$ km relatively to the omnidirectional case (from 6.803 to 10.808 Mbps).

However, for $R = 3$ km, the impact of noise is higher. Without sub-channelisation, the improvement is only of $\sim 32\%$ (from 5.886 to 7.756 Mbps). Only with the use of sub-channelisation a larger improvement, of $\sim 57\%$, is achieved with sectorization (from 6.751 to 10.605 Mbps).

We learned from this work that there is a need to improve the results for the maximum achieved throughput in the outer coverage rings of the cells as this is the zone that suffers the highest interference. The use of relays within fractional reuse schemes is being pointed out as a solution for this challenge, and this issue needs to be investigated.



Fig. 9 Toolbar on the graphic environment of ArcGIS

4 Wireless Planning Tool

4.1 Framework and Scenario

Models for the achievable physical throughput, cellular coverage, and frequency reuse are very useful for the automation of cellular planning procedures. Cellular planning is highly dependent on the propagation environment and a careful choice of the placement, height and tilt of the BS transmitter antennas is needed in order to ensure a high percentage of LoS within the cells. As a consequence, the use of GIS is needed to account for the terrain profile.

In the context of the MobileMAN project [22], a cellular fixed WiMAX PtM network [1], covering the whole district of Covilhã, and in particular the city area was considered. While the overall cellular structure is mainly dedicated to emergency and security public services urban micro-cells will support e-learning and e-health services, among others.

Although the district of Covilhã area is 550 km², the territorial framework of the frequency band license assigned by ANACOM, the Portuguese regulator, is broader, and includes the whole area under study within the MobileMAN project in Beira Interior, Portugal.

4.2 Functionalities and Potentialities of the WPT

The WPT uses ArcGIS as a working environment and allows for automating the planning. Radio and network characteristics are studied, including the link budget, definition of radio propagation models, and system capacity. The planning tool is made available as a toolbar in ArcGIS allowing the user to choose several system parameters, such as the number of base stations, the number of users, and network different environments, Fig. 9.

The options included into the toolbar are accessed via buttons and include the following WiMAX planning functionalities:

4.2.1 Definition of Urban Zones

With this button urban zones are defined for BSs not working at full power since, as the user density is much higher than in rural areas, the limitation is system capacity rather than radio coverage. Limitations on transmitter power may also arise due to regulatory constraints.

4.2.2 Equipment

There are two buttons that deal with options for the WiMAX equipment. The first enables to choose equipment, according to data provided by its manufacturer, while the second deals with the equipment data. The available equipment can be either from a manufacturer available on the market or customized by the user definitions. In the former case, it is possible to define bandwidth, frequency, and type of antenna. In the latter, the planner may define all the parameters, e.g., bandwidth, transmission power, sensitivity, frequency, and type of antenna.

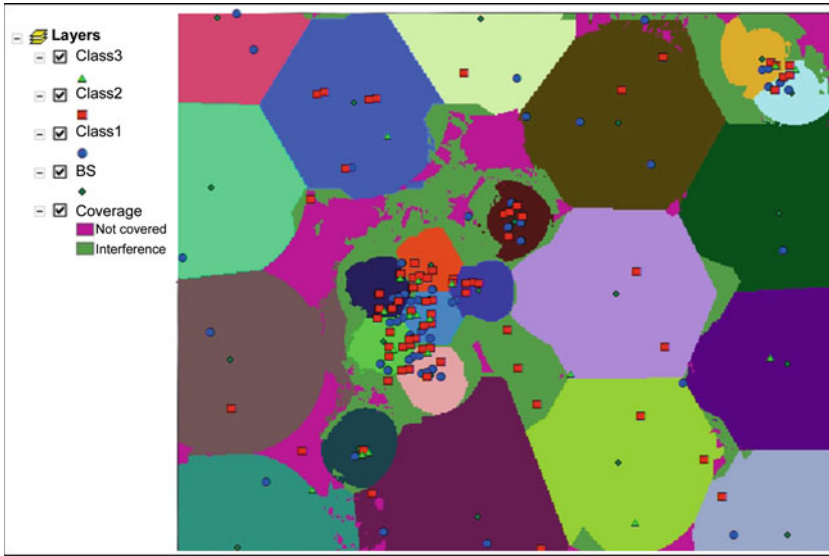


Fig. 10 Map with different kind of users (cells use sectorial antennas to cover the district of Covilhã)

4.2.3 Sites with LoS and NLoS

This option allows for the verification of the existence of LoS, and helps to choose the propagation model to be used on each zone of the map, compute the received power, and analyse the type of application.

4.2.4 Received Power and Coverage

This functionality creates three different layers. One has a coloured map for each value computed for the received power at each point of the map, depicted in Fig. 10. The other shows the values for *CNIR* and, using them, it is possible to check the areas with appropriate coverage and select the capacity option to be used at each point. The remaining layer is a scheme where the different areas covered by each BS, the interference areas, and areas that were not covered are represented.

One of the functionalities of the GIS tool is the creation and superposition of layers (non-line-of-sight versus line-of-sight, received power, *CNIR*, spatial coverage and user positions while supporting different classes of service).

4.2.5 Users

Presents a menu to define the percentage of users in each class, e.g., percentages of users with real time services, and the density of users per km^2 . Figure 10 shows that these users are then randomly distributed on the map, where the different classes are distinguished by different symbols. The three service classes, one, two and three, distinguish real-time applications at 64, 384, and 2000 kbps, respectively. A given percentage of users has access to time-based applications (the ones where the time is an intrinsic component of the application, e.g., voice or video) while others are using non time-based ones. Results include

Table 4 Coverage and interference areas for the district of Covilhã

Propagation model	Type of antenna	Coverage area (%)		Non-covered area (%)
		Without interference	With interference	
SUI-C	Omnidirectional	52.3	42.0	5.7
	Sectorial	85.0	9.3	5.7
Modified friis	Omnidirectional ^a	70.0	0.0	30.0

^a In this case, three 180° BS sectorial antennas were used together with 15 omnidirectional ones

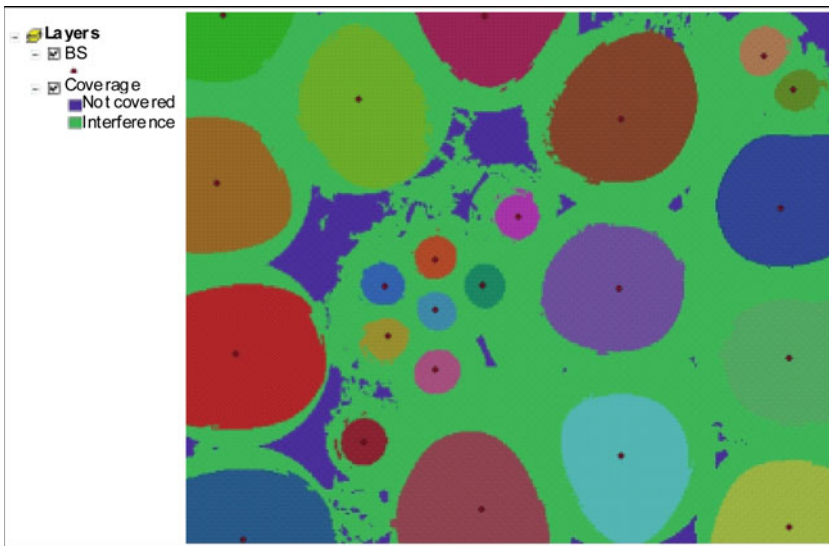


Fig. 11 Use of omnidirectional antennas in the district of Covilhã

the distribution of users by classes, percentage of areas covered and subject to interference, modulation schemes for each BS, number of user at each cell, throughput and percentage of served users. There is an overlay between macro-cells with 3 km radius, and micro-cells with 1 km radius.

4.3 Planning Results

Because the district of Covilhã is very hilly, apart from micro-cells, cells with coverage distances around 3 km are used, differently from the whole region of Beira Interior, where larger cells were considered (up to 5 km), Fig. 10, i.e., micro-cells are overlaid with the macro-cellular structure. The height of BS antennas is 30 m, and the sum of the transmitter and receiver antenna gains is higher than in the experimental setup. Besides, the transmitter power in urban areas is ~18 dB lower than in rural areas. For this set of results, the SUI-C model was considered but the tool also supports the use of the modified Friis model [15, 16], Table 4. Figure 11 presents the case where omnidirectional antennas were used. From Table 4 one can observe that, with sector antennas, the area of interference (i.e., zones where the value

of *CNIR* is below the lowest threshold) is reduced from 42%, in the omnidirectional case, Fig. 11, down to 9.3% in the sector case, Fig. 10, while the covered area (without interference) increases from 52.3 to 85.0%.

In another exercise, where we considered the modified Friis model, one obtained $\sim 70\%$ of LoS coverage of the area.

5 Conclusions

In this paper we describe a PtM demonstrator for fixed WiMAX that provided measurements for cellular coverage in the suburban area of Covilhã, Portugal. For this zone, and for some distance ranges, by using a curve fitting approach, we conclude that the modified Friis model may be used with a propagation exponent $\gamma = 3$. From the analysis of the results, we also conclude that the Stanford University Interim model may be considered, mainly SUI-C but also SUI-B, as the mean square error is reasonable.

From the analysis of *CNIR*, it is clear that noise and interference present a strong limitation to the performance of fixed WiMAX mainly for higher order modulation and coding schemes. With a reuse pattern $K = 7$, cell throughputs near the maximum are only achieved in the UL if sub-channelisation is used together with sectorization. With the use of sub-channelisation alone, although noise power decreases, the improvement only allows for balancing the physical throughputs between the UL and DL for $R = 3$ km (but not achieved for $R = 2$ km).

For low coverage distances, the use of sectorization alone in the UL allows a substantial gain in the physical throughput. However, for larger coverage distances, in the absence of sub-channelisation the achieved gain is not comparable with the case where sub-channelisation is present.

In general terms, the use of sectorization in fixed WiMAX allows for reducing the reuse pattern while considering sub-channelisation allows for improvements on the coverage. The reduction of the reuse pattern corresponds to an increase in system capacity but the improvements in the coverage range (through sub-channelisation) can also allow for an indirect improvement in system capacity, as adaptive MCSs are used.

Some improvements were made in the previous tool, the so-called WPT [4], which allows for a planning designer to dimension WMAN topologies via a practical approach. It is possible to obtain the signal coverage and throughput maps from the plan of a given zone. Hence, this tool constitutes a simple and complete way to implement the most recent WMAN solutions. Besides, it also produces budget planning. LoS dimensionings, based in GIS, were addressed, and applications to rural and sparse urban areas were presented. One important conclusion is the need for sectorial antennas to guarantee an adequate coverage and interference mitigation for several terrain types and environments, including hilly terrains.

Future research directions motivated by the need to improve the results for the maximum achieved throughput in the outer cell coverage rings as this is the zone that suffers the highest interference. The use of relays within fractional reuse schemes can be a solution to answer to this challenge.

Acknowledgments This work was partially funded by MobileMAN (Mobile IP for Broadband Wireless Metropolitan Area Network), an internal project from Instituto de Telecomunicações/ Laboratório Associado, by CROSSNET (Portuguese Foundation for Science and Technology POSC project with FEDER funding), by “Projecto de Re-equipamento Científico” REEQ/1201/EEI/ 2005 (a Portuguese Foundation for Science and Technology project), and by the Marie Curie Intra-European Fellowship OPTIMOBILE (Cross-layer Optimization for the Coexistence of Mobile and Wireless Networks Beyond 3G, FP7-PEOPLE-2007-2-1-IEF). The authors acknowledge the fruitful contributions on ArcGIS tools from Eng.º José Romão, Eng.º José Riscado

and Prof. Victor Cavaleiro from STIG-UBI, and the contribution given by the final year project students in several programming and measurement tasks. Authors also acknowledge the fruitful discussions within COST 2100, a cooperation Action on Pervasive Mobile & Ambient Wireless Communications. Fernando J. Velez acknowledges the fruitful discussions with Prof. Hamid Aghvami. Special thanks are due to Prof. Carlos Salema who helped us in the final revision of the manuscript.

References

1. Liu, H., & Li, G. (2005). *OFDM-based broadband wireless networks—design and optimization*. Hoboken, New Jersey, USA: Wiley.
2. IEEE. (2009). *IEEE standard for local and metropolitan area networks—part 16: Air interface for fixed broadband wireless access systems*. New York, NY, USA: IEEE Std 802.16-2009 (Revision of IEEE Std 802.16-2004), IEEE.
3. IEEE. (2006). *IEEE standard for local and metropolitan area networks—Part 16: Air interface for fixed and mobile broadband wireless access systems—amendment 2: Physical and medium access control layers for combined fixed and mobile operation in licensed bands and corrigendum 1*. New York, NY, USA: IEEE Std 802.16e-2005 and IEEE Std 802.16-2004/Cor 1-2005 (Amendment and Corrigendum to IEEE Std 802.16-2004), IEEE.
4. Tomé, R., Lourenço, P., Grilo, A., Cercas, F. C., Rodrigues, A. J., Velez, F. J., et al. (2005). A WLAN planning tool with a practical approach. In *Proceedings of International Symposium on Wireless Personal Multimedia Communications WPMC* (Vol. 2, pp. 1286–1290). Denmark: Aalborg.
5. IEEE. (1999). *Part II: Wireless LAN media access control (MAC) and physical layer (PHY) specifications*. New York, NY, USA: IEEE Std 802.11-1999, IEEE.
6. Fragoso, J. G., & Tejada, G. M. G. (2005). Cell planning based on the WiMax standard for home access: A practical case. In *Proceeding of 2nd ICEEE and XI CIE 2005* (pp. 89–92). Mexico.
7. Ibrahim, A. H., Ismail, M., Kiong, T., & Mastan, Z. (2005). Development of software planning tools for an-intelligent traffic light wireless communication link using 5.8GHz WLAN. In *Proceeding of 2005 Asia-Pacific Conference on Applied Electromagnetics* (pp. 378–382). Malaysia: Johor.
8. Ruiz, S., Samper, Y., Pérez, J., Agusti, R., & Olmos, J. (1998). Software tool for optimising indoor/outdoor coverage in a construction site. *Electronics Letters*, *34*(22), 2100–2101.
9. Wertz P., Sauter M., Wölflé G., Hoppe R., & Landstorfer F. (2004). Automatic optimization algorithms for the planning of wireless local area networks. In *Proceeding of VTC 2004-Fall, IEEE 60th Vehicular Technology Conference 2004-Fall-Wireless Technologies for Global Security* (pp. 3010–3014). Los Angeles, CA, USA.
10. Anderson, H. R. (2003). *Fixed broadband wireless systems design*. Chichester, West Sussex, UK: Wiley.
11. Erceg, V., et al. (1999). An empirically based path loss model for wireless channels in suburban environments. *IEEE Journal of Selected Areas in Communications*, *17*(7), 1205–1211.
12. IEEE 802.16 Working Group. (2001). *Channels models for fixed wireless applications*. Document 802.16.3c-01/29r4.
13. Hari, K. (2000). *Interim channel models for G2 MMDS fixed wireless applications*. Tampa, USA: IEEE 802 plenary meeting.
14. Wahl, R., Stäbler, O., & Wölflé, G. (2007). Propagation model and network simulator for stationary and nomadic WiMAX networks. In *Proceeding of IEEE VTC 2007 Fall-IEEE 66th Vehicular Technology Conference*. Baltimore, MD, USA.
15. Rappaport, T. S. (2002). *Wireless communications: Principles and practice*. Upper Saddle River, NJ, USA: Prentice Hall.
16. Moldkar, D. (1991). Review on radio propagation into and within buildings. In *Proceeding of IEE Microwaves, Antennas and Propagation*, (Vol. 138, No.1, pp. 61–73).
17. Panagopoulos, A. D., Arapoglou, P.-D. M., Kanellopoulos, J. D., & Cottis, P. G. (2007). Inter-cell radio interference studies in broadband wireless access networks. *IEEE Transactions on Vehicular Technology*, *56*(1), 3–12.
18. Sari, H. (2001). A multimode CDMA with reduced intercell interference for broadband wireless networks. *IEEE Journal on Selected Areas in Communications*, *19*(7), 1316–1323.
19. Bauer, G., Bose, R., & Jakoby, R. (2005). Three-dimensional interference investigations for LMDS networks using an urban database. *IEEE Transactions on Antennas and Propagation*, *53*(8), 2464–2470.
20. Velez, F. J., Correia, L. M., & Brázio, J. M. (2001). Frequency reuse and system capacity in mobile broadband systems: Comparison between the 40 and 60GHz bands. *Wireless Personal Communications*, *19*(1), 1–24.

21. Velez, F. J., Carvalho, V., Santos, D., Marcos, R. P., Costa, R., Sebastião, P., et al. (2005). Planning of an IEEE 802.16e network for emergency and safety services. In *Proceeding of 3G 2005-6th IEEE International Conference on 3G Mobile Communication Technologies* (pp. 507–511). London, UK.
22. <http://www.e-projects.ubi.pt/mobileman/>.

Author Biographies



Pedro Sebastião (S'95-M'05) received the BSc degree in Electronics, Telecommunications and Computing from ISEL, Polytechnic Institute of Lisbon, Portugal, in 1992. He received his Licenciado and MSc degrees in Electrical and Computer Engineering from IST, Technical University of Lisbon, in 1995 and 1998, respectively. He worked for Department of Studies and Innovation in the Portuguese Defence Industries (1992–98), Department of Business Communication in Siemens (1999–2005), and ISG, a High Education Business School, as a lecturer (1999–2005). In 2005 he joined LUI-ISCTE, where he is a lecturer. He is a research assistant at Instituto de Telecomunicações since 1995. He has been involved on several research projects and his interests include planning tools for Wi-Fi and WiMAX, stochastic models and efficient simulation algorithms for physical layer. He is a member of IEEE, Sociedade Brasileira das Telecomunicações and Ordem dos Engenheiros.



Fernando José Velez received the Licenciado, MSc and PhD degrees in Electrical and Computer Engineering from Instituto Superior Técnico, Technical University of Lisbon in 1993, 1996 and 2001, respectively. Since 1995 he has been with the Department of Electromechanical Engineering of University of Beira Interior, Covilhã, Portugal, where he is Assistant Professor. He is also researcher at Instituto de Telecomunicações, Lisbon. He made or makes part of the teams of RACE/MBS, ACTS/SAMBA, COST 259, COST 273, COST 290, IST-SEACORN, IST-UNITE, and COST 2100 European projects, he participated in SEMENTE and SMART-CLOTHING Portuguese projects, and he was the coordinator of four Portuguese projects: SAMURAI, MULTIPLAN, CROSSNET, and MobileMAN. He has authored five book chapters, around seventy five papers and communications in international journals and conferences, plus twenty five in national conferences, and is a senior member of IEEE and Ordem dos Engenheiros (EUREL), and a member of IET and IAENG. His main research areas are cellular planning tools, traffic from mobility, simulation of wireless networks, cross-layer design, interworking, multi-service traffic and cost/revenue performance of advanced mobile communication systems.



Rui Costa was born in Santarém, Portugal, and received the Licenciado degree in Informatics from Instituto Matemáticas e Gestão-Universidade Lusofona in 1999. He is the responsible by the development and management of the Computer Services and network of the Health Sciences Faculty of University of Beira Interior, he works on the development of wireless LAN, MAN and WAN, e-Learning, b-Learning and m-Learning applications, advanced WIA (wireless Internet applications), RIA (rapid Internet applications) in University environments for Web2. He is concluding his MSc on cellular planning and deployment issues for fixed and portable WiMAX.



Daniel Robalo received the Licenciado and MSc degrees in Electrical Engineering from University of Beira Interior (UBI), Covilhã, Portugal, in 2005 and 2008, respectively. His MSc research was done in the context of the MobileMAN project, an internal project on WiMAX deployment from Instituto de Telecomunicações (IT). He is currently a researcher at IT, and his research interest is in the field of Broadband Wireless Access, including design and implementation of WiMAX networks. Besides conference papers, including IEEE ones, he has two journal papers and one book chapter accepted for publication.



António Rodrigues received the B.S. and M.S. degrees in electrical and computer engineering from the Instituto Superior Técnico (IST), Technical University of Lisbon, Lisbon, Portugal, in 1985 and 1989, respectively, and the Ph.D. degree from the Catholic University of Louvain, Louvain-la-Neuve, Belgium, in 1997. Since 1985, he has been with the Department of Electrical and Computer Engineering, IST, where is currently an Assistant Professor. His research interests include mobile and satellite communications, wireless networks, spread spectrum systems, modulation and coding.